Preprint Title	One-Step Direct Amination of Nanodiamond Surface and Facile Separation by Viscosity Gradient Centrifugation
Authors	Nianshun Yang, Jean Felix Mukerabigwi, Xueying Huang, Yuyang Sun, Juanxiao Cai and Yu Cao
Publication Date	21 Okt 2019
Article Type	Full Research Paper
Supporting Information File 1	Supporting Information.docx; 32.0 KB
ORCID® iDs	Nianshun Yang - https://orcid.org/0000-0002-3362-9812; Jean Felix Mukerabigwi - https://orcid.org/0000-0002-5013-2963; Yu Cao - https://orcid.org/0000-0002-3362-9812

One-Step Direct Amination of Nanodiamond Surface and Facile Separation by Viscosity Gradient Centrifugation

Nianshun Yang[1] [+], Jean Felix Mukerabigwi[1], Xueying Huang[1], Yuyang Sun[1], Juanxiao Cai[1], Yu Cao[1][*][+]

Key Laboratory of Pesticide and Chemical Biology (Ministry of Education), College of Chemistry,

Central China Normal University, Wuhan 430079, P. R. China

* Corresponding author.

Prof. Yu Cao, Tel: +86-27-61311087, Fax: +86-27-67867141, E-mail: caoyu@mail.ccnu.edu.cn.

Abstract: The introduction of terminal amine functional group on nanodiamond (ND) surface has been proposed as the key strategy to enable further synthesis of various ND derivatives for a wide range of application including sensors and biomedicine. Nevertheless, it is still challenging to develop a successful synthesis procedure to achieve monodispersed ND-NH$_2$ mostly due to the undesirable high agglomeration effect of ND particles and complex synthetic steps which dramatically limit their practical use. In this work, we demonstrate a facile approach to obtain the direct amination of the ND surface, through a one pot mechanochemical reaction using ball milling in the presence of NH$_4$Cl. To obtain monodispersed ND-NH$_2$, a straightforward process by virtue of viscosity gradient centrifugation is adopted using aqueous polyvinylpyrrolidone (PVP) and glycerol. The results show a successful synthesis of ND-NH$_2$ as evidenced by FT-IR and ζ–potential analysis. Moreover, the aminated ND particles morphology and size distribution analysis by TEM and DLS, respectively, show that using viscosity gradient built from aqueous PVP can achieve a better separation of NDs by size. Therefore, the findings suggested that the application of mechanochemical reactions and viscosity gradient centrifugation can be used to achieve homogeneous and monodispersed functionalized NDs for further specific technical applications. **Keywords:** viscosity gradient; centrifugation; nanodiamonds; polyvinylpyrrolidone; mechanical reaction

1. Introduction

NDs is a novel carbon nanomaterial with good chemical stability [1], low toxicity [2], and good biocompatibility [3]. The aminated surface of the ND is of high interest, as it would enable the straightforward binding of a large variety of functional molecules, which leads to a wide range of applications for NDs including sensors and biomedicine [4-6].

According to different methods for de-agglomeration of NDs, there are many methods for surface modification of ND particles. The common methods include surface chemical modification

and mechanochemical modification. At present, there are two methods for obtaining nanoparticles having a narrow size distribution and uniform morphology. The first is the direct synthesis of such nanoparticles [7-10]; The second is the separation of the prepared nanoparticles having a broader particle size distribution. Among them, the surface chemical modification method and mechanochemical modification method of ND are the first method. However, the direct amination of the ND surface turned out to be rather difficult. Until now, the direct grafting of amino groups onto the surface of ND was not fully successful, which generally requires harsh environments and complex synthesis steps. For example, Krueger et al [11] used aminated silane to functionalize ND surface and obtain aminated ND. Mochalin et al [12] used $SOCl_2$ to react with functional groups on the surface of ND, first obtaining ND-COCl, and then reacting with ethylenediamine to obtain ND-NH_2. HX Hu and teammates [13] realized an efficient strategy by functionalized ND with biodegradable Polyurethane (PU) for ND surface modification. Nevertheless, it actually remains amination process is cumbersome and cannot be a one-step amination. Although mechanochemical reactions using ball milling approach does not require high temperature conditions and complicated synthesis steps, which depend on several parameters like milling frequency, milling time , size and number of milling balls, and the material of milling balls and beakers. It can be seen that for the preparation method based on the existing direct synthesis, a harsh synthetic environment and time-consuming optimization of industrial parameters are usually required, which make it difficult to directly achieve strict size control of the NDs. Therefore, there is an urgent need to develop a low-cost, high-efficiency preparation of monodisperse NDs.

Recently, density gradient centrifugation has a high degree of controllability due to the separation system. It is universal and efficient for the separation and purification of nanomaterials with different morphologies, different sizes and different synthetic systems, and becomes an efficient

separation method for nanomaterials [14-18]. Large nanoparticles are usually denser than liquid media and are therefore suitable for separation by differences in settling velocity [19-21]. However, since the density gradient is produced by a superposition solution of compounds of different concentrations, in practice such a change in viscosity is almost inevitable in the process of preparing a density gradient. Qiu et al [22] successfully separated Au and Fe_2O_3 nanoparticles of different sizes by using the viscosity gradient of PVP aqueous solution. It can be seen that the viscosity gradient centrifugation can also effectively separate nanoparticles of different sizes.

Taking these considerations into account, we used mechanochemical reactions using ball milling approach to functionalize ND and achieve one-step the direct amination of the ND surface. In addition, we systematically investigate how the two common viscosity gradient aqueous PVP and glycerol influence separation of NDs. Analysis of the resulting viscosities, TEM, DLS and UV show that wrapping by viscosity gradient built from aqueous the surfactant PVP is necessary to obtain monodisperse NDs. This simple method was also shown as a general method for separation of different type of NDs (such as carboxylated NDs).

1. Experiment

2.1 Materials

All commercial reagents were used without further purification. Pristine nanodiamond (ND, the purity $\geq$ 95%), manufactured by the detonation technique, was obtained from Hebei Satellite Chemical Co., Ltd., China. PVP (average molar mass =8000) was obtained from Aladdin.

2.2 Characterization

For the FT-IR test of the various ND samples were obtained from KBr pellets using IR-960. The ζ–potential dynamic was conducted at room temperature using a Malvern-ZS90 potentiometer. Transmission electron microscopic (TEM) images were performed on a JEM-2100F microscope

operating at 200 kV accelerating voltage. The size distribution of samples obtained from different gradient fractions were measured through dynamic light scattering analyzer (DLS, WYATT, DynaPro NanoStar). The optical properties of fractions were characterized by UV-Vis absorbance spectroscopy (Cary60 UV-Vis).

2.3 Synthesis of ND-COOH

Pristine ND (5.0 g) was suspended in $HClO_4$. The mixture was magnetic stirred at room temperature for 3 h, followed by slowly heating to 493 K, with heating rate less than 278 K / 5 min, and then allowed to stir for another 4 h at 493 K. The reaction mixture was then cooled to room temperature, diluted with deionized H_2O, separated by centrifugation and washed until the pH value of the supernatant liquor arrived to about 6. Finally，the sample was dried in an oven at 333 K for 24 h to obtain ND-COOH.

2.4 Synthesis of ND-NH$_2$

Ball Milling conditions: 0.5 g ND-COOH, 5 g NH_4Cl, 5 g milling auxiliary (NaCl); milling beakers (V_{MV} =100 mL) and milling balls made from Yttrium-stabilized zirconia (YSZ); planetary ball mills (PBM, QM-1SP2, Nanjing University Instrument Factory, China) P7 classic line , t =2 h, rpm = 420 min . After the ball milling is completed, the reaction was taken out, diluted with deionized H_2O, separated by centrifugation. The above operation was repeated about 2-3 times to obtain amination of the ND surface (ND-NH$_2$).

2.5 Preparation of viscosity gradient

Two different viscosity gradient aqueous PVP and glycerol were adopted to separate NDs respectively, all of which were formed in a centrifuge tube with 15 mL Beckman centrifuge tubes (polycarbonate, diameter 13 mm, length 120 mm). All separation experiments were performed on an AXT16G Beckman ultracentrifuge (298 K, centrifugal force of 1645 g). Case I: it was built up by 2,

4, 6, 8, and 10 wt% aqueous PVP. Case II: it applied by using 6.5, 13.5, 17.5, 23.0, and 28.5 wt%

aqueous glycerol as viscosity gradients, whose viscosities are equivalent to 2, 4, 6, 8, and 10 wt%

aqueous PVP, respectively.

2.6 Centrifugal separation of ND-NH$_2$

Approximately 0.8 mL of ND-NH$_2$ in 0.1 wt % aqueous dispersion was placed on top of case I

and Case II, respectively, and then centrifuged at 1645 g for 3 h. After the centrifugation, four

fractions of NDs were taken from tube in a unit of 0.4 mL using a micropipette, which were

characterized by TEM, UV and DLS.

2.7 Centrifugal separation of ND-Ox

We also used air oxidation at 693 K to compare carboxylated ND (ND-Ox), which size widely

distributed between 122.3–279.5 nm, with a mean dimension of 122.3 nm（**Figure S1**）. Here we

made our attempt to separate ND-Ox in the PVP viscosity gradient (case I).The experimental

conditions were the same as the conditions for separating ND-NH$_2$. After the centrifugation, the

samples were characterized by TEM, UV and DLS.

3. Results and discussion

3.1 FT-IR characterizations

The FTIR spectra of pristine ND, ND-COOH and ND-NH$_2$ are compared in **Figure 1**. The FT-

IR of pristine ND show a peak at 3428 cm^{-1} corresponding to the stretching of O-H band from trace

of water that attaches on ND surface [23]. The appearance of hydroxyl group 1628 cm^{-1} identifies the

existence of hydroxyl groups on pristine ND surface. In contrast with that of pristine ND in **Figure

1**a, the displacement of the band at 3428 cm^{-1} in **Figure 1**b for ND-COOH is related to the loss of

water molecules. The peak at 1798 cm^{-1} attributed to the stretching of the C═O bond of the carboxylic

acid is sharper than pristine ND. In the **Figure 1**c, the highly intense band observed at 1628 cm-1 is

attributable to the so-called "amide I" band that is characteristic of all amides and originates from the stretching of the C=O bond. In addition, the peak at $3428cm^{-1}$ is attributed to the N-H stretching band, and the existence of C-N deformation vibration band at $1108cm^{-1}$ prove that the formation of covalent bonds between NH_4Cl and ND-COOH.

3.2 ζ–potential characterization

The ζ–potentials of ND-COOH (**Figure 2**, black line) and ND-NH$_2$ (**Figure 2**, red line) are shown in **Figure 2**. When pH is increased, the ζ–potentials of ND-COOH and ND-NH$_2$ become more negative. The ζ–potential shifts to a negative value and the absolute value gradually increases, which means the dispersion stability gradually increases. **Figure 2** (black line) shows ζ-potential of ND-OOH is maximum about -42.8 mV at pH = 10, because the ionization equilibrium ND-COOH $\rightleftharpoons$ ND-COO$^-$ + H$^+$ shifts to the right when the pH increases, resulting in ζ–potential of ND-COOH is gradually increased, and the dispersion stability is also gradually increased. Owing to the surface of ND-NH$_2$ that has both carboxylic and amino groups, ND-NH$_2$ is an amphoteric material. **Figure 2** Shows ζ-potential of ND-NH$_2$ are more negative than ND-COOH, because of dissociation of the amino group of ND-NH$_2$ under alkaline conditions. These results demonstrated that the amino was successfully introduced on the surface of ND.

3.3 TEM morphology analysis

Figure 3 shows that ND-NH$_2$ has good dispersibility, but the particle size range is widely distributed, the small particles sizes are < 10 nm, and the largest particles sizes are > 100 nm. And there is a certain agglomeration phenomenon. The DLS (**Figure S2**) also shows that the average particle size and size distribution was 40.8 nm (33.8 nm - 160.0 nm) respectively, where the smaller particles sides are < 10 nm, but the content are low.

3.4 Separation of ND-NH$_2$ by PVP viscosity gradient centrifugation

Figure 4A shows a photograph of before (a) and after (b) centrifugation of the centrifuge tube by PVP viscosity gradient. The size distribution (**Figure 4**B) of the four typical fractions based on DLS characterization shows that the mean size of f1, f3, f5, and f7 are about 32.8 nm, 48.3 nm, 72.7 nm, and 117.3 nm, respectively. As shown in **Figure 3**, these nanoparticles were initially different sides of ND-NH$_2$ particles. There is less overlap among particle size distributions, which shows process of PVP viscosity gradient centrifugation is ideal. Furthermore, the TEM (**Figure 4**C) images results also exhibited the increase trend of mean size for the fractions from top to down, which also show that the separated ND-NH$_2$ is little aggregation. The difference in particle size is also confirmed by the shift of the UV maximum absorption peak from 230.0 nm (f1) to 235.0 nm (f7).

The density of the aqueous PVP is only slightly higher than water (1.064 g/cm^3 at 30 wt%) and is very close at different concentrations [24], while the ND density is approximately 1.55 g/cm^3. If you want to build equal density gradient centrifugation, you need compare a higher concentration of aqueous PVP. This leads to very high viscosities, which will make it difficult to post-treat these solutions, and will also affect the dispersion of ND-NH$_2$. Therefore, 2, 4, 6, 8, and 10 wt% of the low mass fraction of the aqueous PVP are selected as the separation gradient, which also facilitates the post-treatment of the experiment. In addition, 10 wt% of PVP is only about 1.7% larger than the 2 wt% solution density and there is only about a 1% difference between adjacent layers (**Table S1**, Supporting Information). However, the viscosity change between the PVP gradient layers varies greatly compared to the density. The viscosity of the 10 wt% PVP solution is approximately 2 times higher than the viscosity of the 2 wt% PVP solution, and the viscosity change between adjacent layers is between 1.1 and 1.2 times (**Table S1**, supporting information). Since the density of ND is larger than that of the gradient medium, the separation of ND-NH$_2$ in the PVP gradient belongs to the rate zone centrifugal separation, which is by the settling velocity difference among large- and small-sized

NDs, rather than the density difference.

Theoretically, according to the classical deposition theory [25], the sedimentation velocity v of the colloidal particles in the dispersion medium can be expressed as (Eq. 1).

$$v = 2(\rho_p - \rho_s) \cdot r^2 \, g' \, / \, (9\eta_s) \qquad (1)$$

Where v is the sedimentation velocity of the colloidal nanoparticles, ρ_p and ρ_s are the nanoparticles and PVP aqueous solution, r is the radius of the nanoparticles, g' is the centrifugal force, and η_s is the viscosity of the gradient medium. Since the phase difference between the ND particles density (ρ_p) and the PVP aqueous solutions gradient (ρ_s) does not change much, the separation effect depends on the nanoparticle size, centrifugal force and viscosity. The Aqueous PVP as a separation gradient has two contributions to the precise division of the ND-NH$_2$ size. First, the viscosity between the PVP layers changes greatly, and the density between adjacent layers does not change much, which is equivalent to build pure viscosity gradient. According to Eq.1, when the density and radius of the nanoparticles are constant, this contributes to high separation accuracy. Second, PVP as a surfactant, contributes to the dispersion of ND-NH$_2$. Because PVP surfactant can wet ND-NH$_2$ particles, it is well known that wetting is the most basic condition for solid particle dispersion. If the solid particles are to be uniformly dispersed in the medium, it must first be that each solid particle can be fully wetted by the medium. In addition, since the PVP surfactant can wrap on the surface of ND-NH$_2$, which not only increases the barrier against the re-aggregation of ND-NH$_2$ particles, but also reduces the tension between the ND-NH$_2$ and the PVP aqueous solution. Therefore, the thermodynamic stability system of the dispersion system is increased. The viscosity gradient from PVP aqueous solutions centrifugation provided an easy and effective way of separating different sides of ND-NH$_2$ during the process.

3. 5 Separation of ND-NH$_2$ by glycerol viscosity gradient centrifugation

In order to compare the advantages of the previous PVP aqueous solutions as a viscosity gradient, here we select the common water-soluble small molecule organic glycerol aqueous solutions as a gradient medium. We attempted to use 6.5, 13.5, 17.5, 23.0, and 28.5 wt% aqueous glycerol solutions as viscosity gradients corresponding to 2, 4, 6, 8, and 10 wt% PVP aqueous solutions, respectively. Moreover, the viscosity among the glycerin gradient layers also changes greatly, and densities are very close to each other among different concentrations (**Table S2**).

Figure 5A shows a digital photograph of before (a) and (b) after centrifugation of the centrifuge tube by glycerol viscosity gradient. The size distribution (**Figure 5**B) of the four typical fractions based on DLS characterization shows that the mean size of 34.9 nm, 128.7 nm, 194.1 nm, and 615.8 nm, respectively (f9-f15).These particles size distribution range are wider and overlap more, and the separated ND-NH$_2$ particles aggregate micro-sized clusters. The TEM images (**Figure 5**C) also prove that the particle size also gradually increased from top to bottom (**Figure 5** f9-f15), but after f11, the aggregation between the particles is severe. It may be that when the ND-NH$_2$ particles pass through the glycerol viscosity gradient, the glycerol can not wet and wrap the ND-NH$_2$ particles like the PVP surfactant, which causes the aggregation among the particles and prevent effective NDs separation.

3.6 Separation of ND-Ox by PVP viscosity gradient centrifugation

The DLS (**Figure 6**B) results exhibit the uniform size distribution for the fractions, which the mean side of f2, f4, f6, and f8 are about 92.3 nm, 131.6 nm, 156.3 nm, and 200.9 nm, respectively. The TEM images (**Figure 6**f2-f8) also prove that. In addition, the shift of the UV maximum absorption peak of **Figure 6**D from 229.0 nm (f2) to 234.5 nm (f8) also confirmed the difference in size among the ND particles after separation. It can be seen that The PVP viscosity gradient can separate ND-NH$_2$ with average size at 43.88 nm, but also applies to seperate ND-Ox having a larger

average size of 150.3 nm.

4. Conclusions

In this research, mechanochemical reactions in a ball mill is adopted to functionalize ND with NH$_4$Cl to functionalize ND to obtain the direct aminated ND surface. The functionalized NDs were characterized by various techniques, which show that amino group had been successfully introduced on surface of ND. Moreover, we have successfully obtained relatively homogeneous and monodisperse NDs by a facile PVP viscosity gradient centrifugation. The present separation method by centrifugation of NDs is simple, rapid and effective. The settling velocity difference is related to the size or shape and density of the NPs, which is not depended on their other physical or chemical properties [25]. Thus, although we only used ND-NH$_2$ and ND-COOH particles in the experimental demonstrations, the PVP viscosity gradient may be used for separation of other functionalization of the NDs with different sides.

References

[1] A. Krueger, Diamond nanoparticles: Jewels for chemistry and physics, Advanced Materials 20(12) (2008) 2445-+.

[2] A.M. Schrand, H. Huang, C. Carlson, J.J. Schlager, E. Osawa, S.M. Hussain, L. Dai, Are diamond nanoparticles cytotoxic?, Journal of Physical Chemistry B 111(1) (2007) 2-7.

[3] N. Mohan, C.-S. Chen, H.-H. Hsieh, Y.-C. Wu, H.-C. Chang, In Vivo Imaging and Toxicity Assessments of Fluorescent Nanodiamonds in Caenorhabditis elegans, Nano Letters 10(9) (2010) 3692-3699.

[4] P.A.I. Purtov K V , Burov A E , et al, Nanodiamonds as Carriers for Address Delivery of Biologically Active Substances[J], Nano Scale Research Letters 5(3) (2010).

[5] J.R. Maze, P.L. Stanwix, J.S. Hodges, S. Hong, J.M. Taylor, P. Cappellaro, L. Jiang, M.V.G. Dutt, E. Togan, A.S. Zibrov, A. Yacoby, R.L. Walsworth, M.D. Lukin, Nanoscale magnetic sensing with an individual electronic spin in diamond, Nature 455(7213) (2008) 644-U41.

[6] A. Alhaddad, M.-P. Adam, J. Botsoa, G. Dantelle, S. Perruchas, T. Gacoin, C. Mansuy, S. Lavielle, C. Malvy, F. Treussart, J.-R. Bertrand, Nanodiamond as a Vector for siRNA Delivery to Ewing Sarcoma Cells, Small 7(21) (2011) 3087-3095.

[7] S.H. Sun, C.B. Murray, D. Weller, L. Folks, A. Moser, Monodisperse FePt nanoparticles and ferromagnetic FePt nanocrystal superlattices, Science 287(5460) (2000) 1989-1992.

[8] X. Wang, Y. Li, Monodisperse nanocrystals: general synthesis, assembly, and their applications, Chemical Communications (28) (2007) 2901-2910.

[9] B.L. Cushing, V.L. Kolesnichenko, C.J. O'Connor, Recent advances in the liquid-phase syntheses of inorganic nanoparticles, Chemical Reviews 104(9) (2004) 3893-3946.

[10] Y. Yin, A.P. Alivisatos, Colloidal nanocrystal synthesis and the organic-inorganic interface, Nature 437(7059) (2005) 664-670.

[11] A. Krueger, J. Stegk, Y.J. Liang, L. Lu, G. Jarre, Biotinylated nanodiamond: Simple and efficient functionalization of detonation diamond, Langmuir 24(8) (2008) 4200-4204.

[12] V.N. Mochalin, I. Neitzel, B.J.M. Etzold, A. Peterson, G. Palmese, Y. Gogotsi, Covalent Incorporation of Aminated Nanodiamond into an Epoxy Polymer Network, Acs Nano 5(9) (2011) 7494-7502.

[13] H.X. Hu, H.M. Guo, X.Y. Yu, K. Naito, Q.X. Zhang, Surface modification and disaggregation of detonation nanodiamond particles with biodegradable polyurethane, Colloids and Surfaces a-Physicochemical and Engineering Aspects 563 (2019) 302-309.

[14] M.S. Arnold, A.A. Green, J.F. Hulvat, S.I. Stupp, M.C. Hersam, Sorting carbon nanotubes by electronic structure using density differentiation, Nature Nanotechnology 1(1) (2006) 60-65.

[15] X. Sun, S.M. Tabakman, W.-S. Seo, L. Zhang, G. Zhang, S. Sherlock, L. Bai, H. Dai, Separation of Nanoparticles in a Density Gradient: FeCo@C and Gold Nanocrystals, Angewandte Chemie-International Edition 48(5) (2009) 939-942.

[16] K.V. Agrawal, B. Topuz, Z.Y. Jiang, K. Nguenkam, B. Elyassi, L.F. Francis, M. Tsapatsis, M. Navarro, Solution-processable exfoliated zeolite nanosheets purified by density gradient centrifugation, Aiche Journal 59(9) (2013) 3458-3467.

[17] X.H. Qi, M.L. Li, Y. Kuang, C. Wang, Z. Cai, J. Zhang, S.S. You, M.Z. Yin, P.B. Wan, L. Luo, X.M. Sun, Controllable Assembly and Separation of Colloidal Nanoparticles through a One-Tube Synthesis Based on Density Gradient Centrifugation, Chemistry-a European Journal 21(19) (2015) 7211-7216.

[18] R. Oliveira-Silva, M. Sousa-Jeronimo, D. Botequim, N.J.O. Silva, D.M.F. Prazeres, P.M.R. Paulo, Density Gradient Selection of Colloidal Silver Nanotriangles for Assembling Dye-Particle Plasmophores, Nanomaterials 9(6) (2019).

[19] M.S. Arnold, J. Suntivich, S.I. Stupp, M.C. Hersam, Hydrodynamic Characterization of Surfactant Encapsulated Carbon Nanotubes Using an Analytical Ultracentrifuge, Acs Nano 2(11) (2008) 2291-2300.

[20] C.L. Zhang, L. Luo, J. Luo, D.G. Evans, X.M. Sun, A process-analysis microsystem based on density gradient centrifugation and its application in the study of the galvanic replacement mechanism of Ag nanoplates with HAuCl4, Chemical Communications 48(58) (2012) 7241-7243.

[21] Z. Chang, C.Y. Wu, S. Song, Y. Kuang, X.D. Lei, L.R. Wang, X.M. Sun, Synthesis Mechanism Study of Layered Double Hydroxides Based on Nanoseparation, Inorganic Chemistry 52(15) (2013) 8694-8698.

[22] P.H. Qiu, C.B. Mao, Viscosity Gradient as a Novel Mechanism for the Centrifugation-Based Separation of Nanoparticles, Advanced Materials 23(42) (2011) 4880-4885.

[23] H.W. Lu, L.M. Zou, Y.J. Xu, Y.V. Li, Controlled dispersion of multiwalled carbon nanotubes modified by hyperbranched polylysine, Journal of Applied Polymer Science 135(19) (2018).

[24] R. Sadeghi, M.T. Zafarani-Moattar, Thermodynamics of aqueous solutions of polyvinylpyrrolidone, J. Chem. Thermodynamics 36 (2004) 665–670.

[25] H. Lamb. Hydrodynamics. Cambridge University Press. Cambridge; UK 1975.
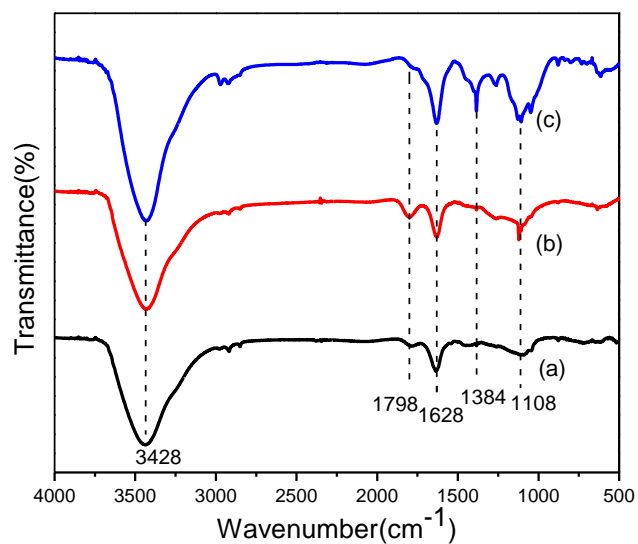
Figure 1. FT-IR spectra of pristine ND (black line a), ND-COOH (red line, b), ND-NH$_2$ (blue line,

C).
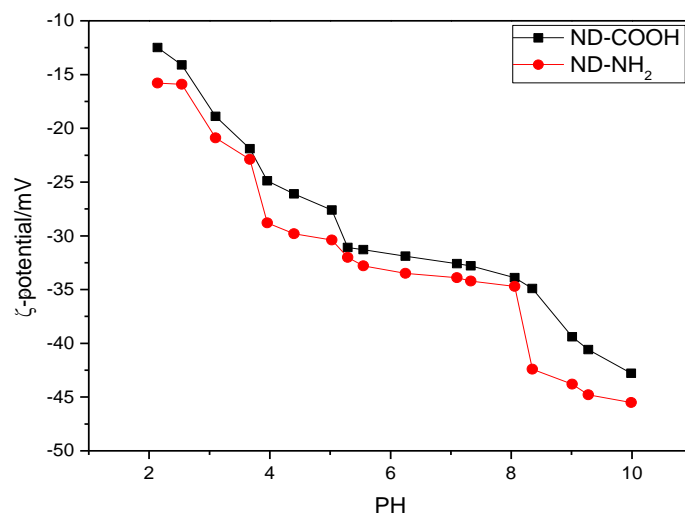
Figure 2. ζ–potential of ND-COOH and ND-NH$_2$ in 0.1 wt % aqueous dispersions as a function of

pH
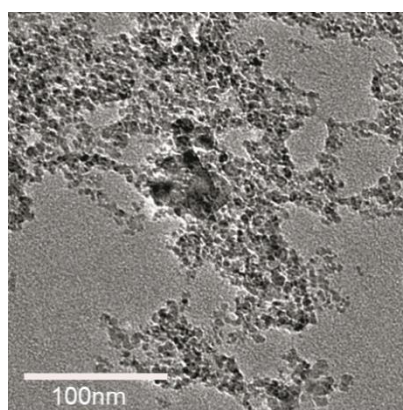
Figure 3. TEM image of the ND-NH$_2$
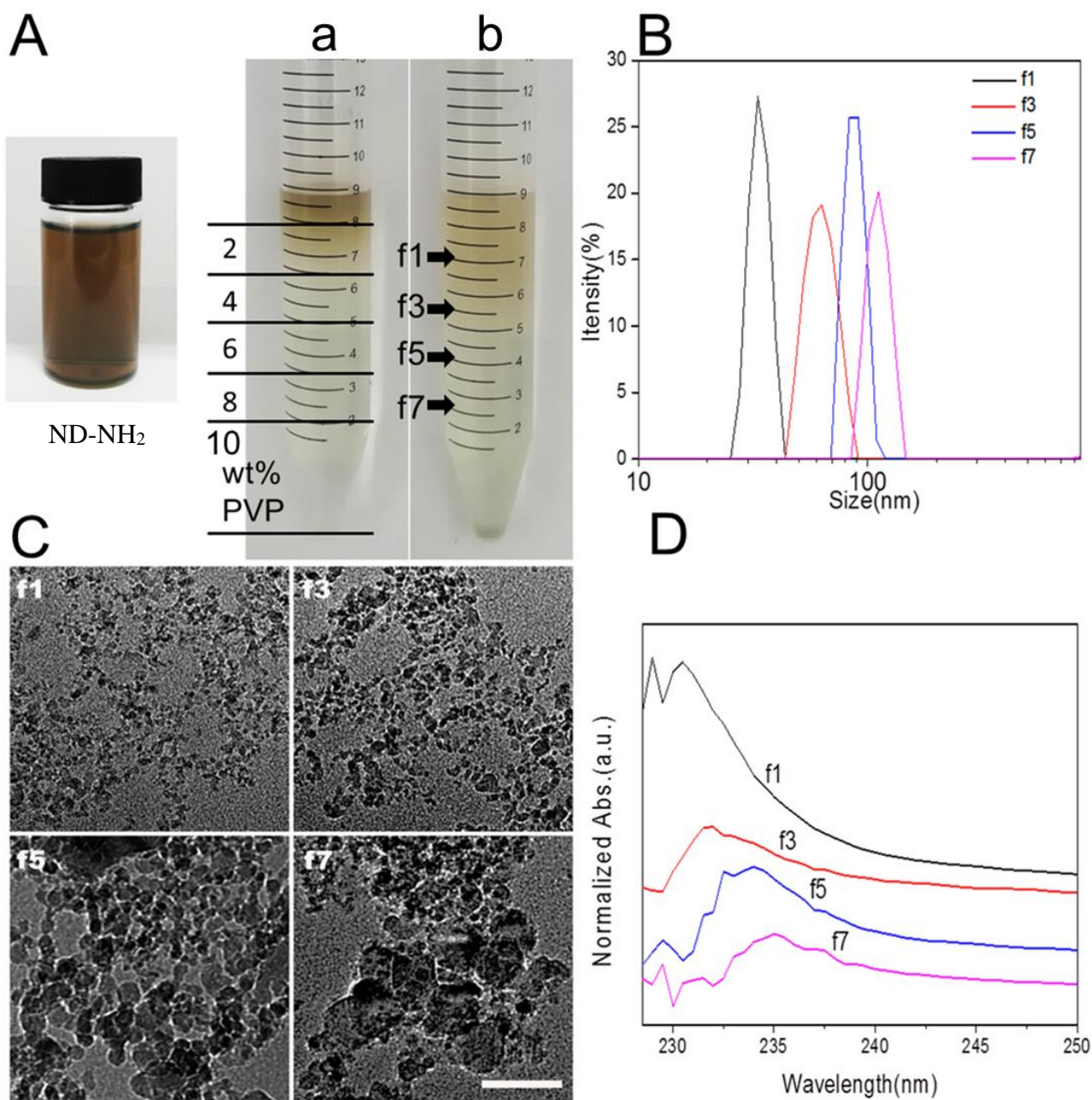
Figure 4. Viscosity gradient was built from aqueous PVP for centrifugal separation of ND-NH₂ particles. Digital photograph of centrifuge tube before and after centrifugation A): a) before separation; b) after separation. B) DLS of four fractions: f1, f3, f5, f7. C) TEM images of the four typical fractions. Scale bar: 50 nm in (f7) is applicable to all images. D) UV-Vis absorption spectra of the four fractions.
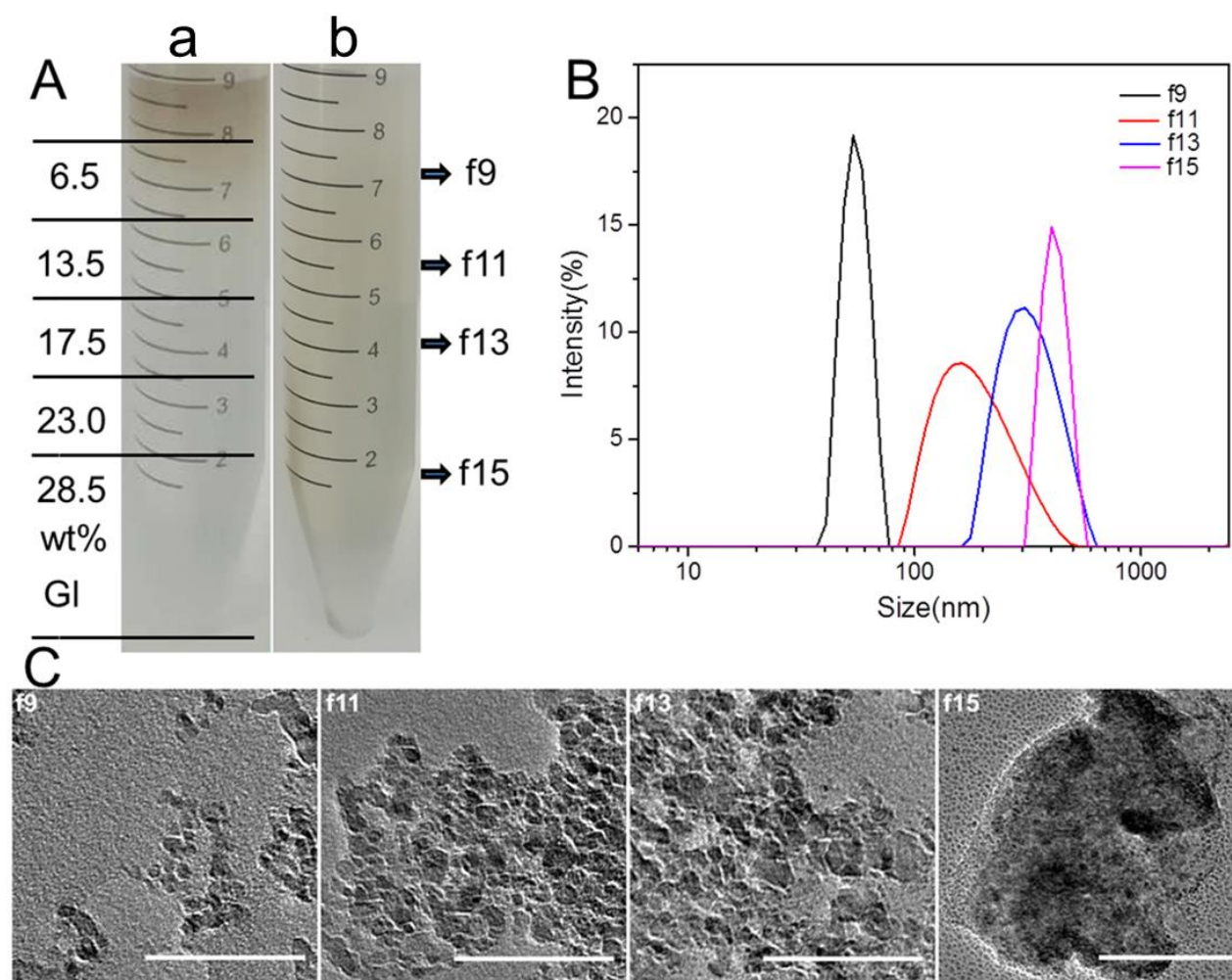
Figure 5. Viscosity gradient was built from aqueous glycerol (Gl) for centrifugal separation of ND-NH$_2$ particles. Digital photograph of centrifuge tube before and after centrifugation A): a) before separation; b) after separation. B) DLS of four fractions: f9, f11, f13, f15. C) TEM images of the four typical fractions. Scale bars: 50 nm in (f9-f13) and 100 nm in (f15).
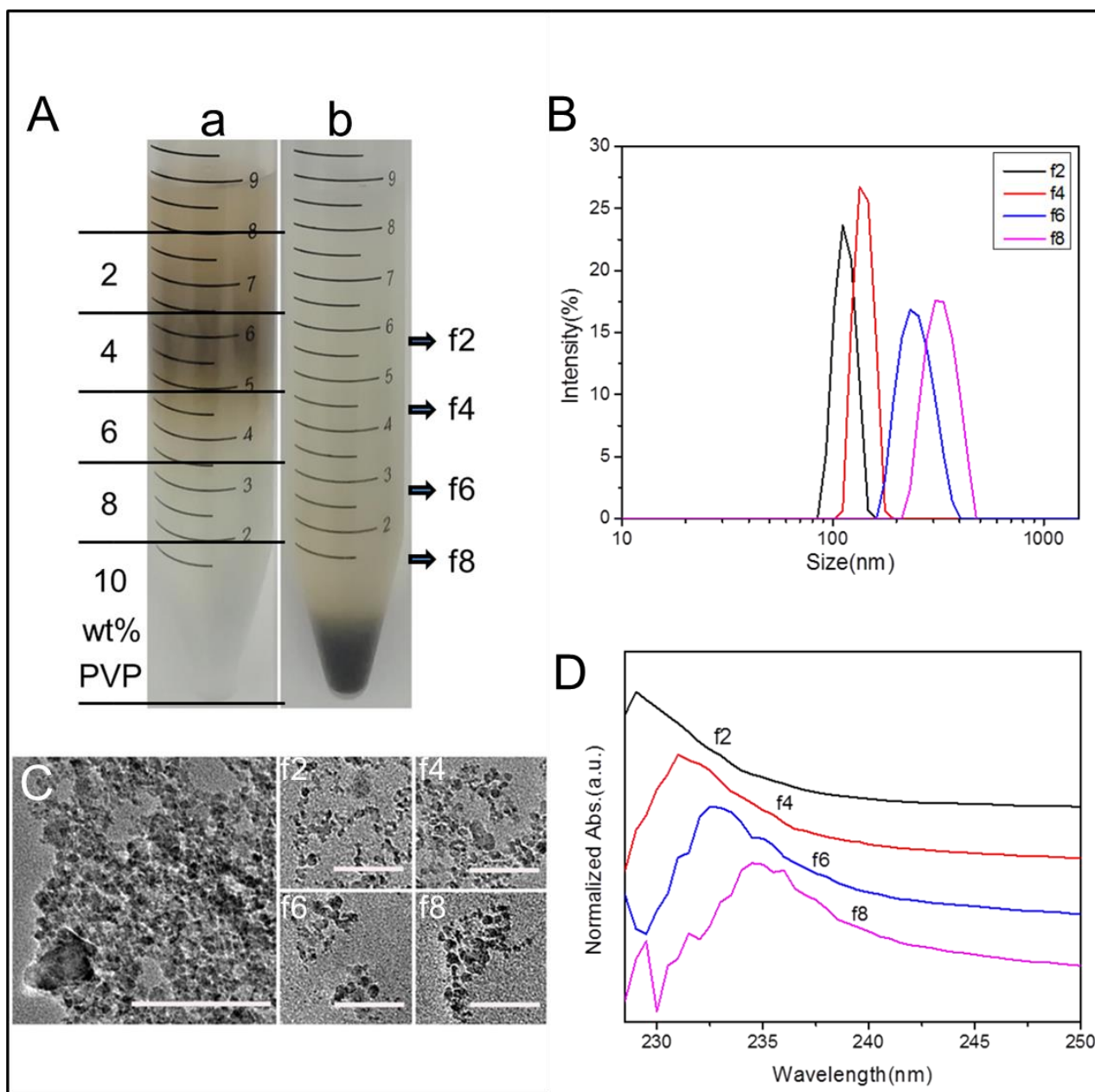
Figure 6. Viscosity gradient was built from aqueous PVP for centrifugal separation of ND-Ox particles. Digital photograph of centrifuge tube before and after centrifugation A): a) before separation; b) after separation. B) DLS of four fractions: f2, f4, f6, f8. C) TEM image of the ND-Ox (scale bar: 100 nm). TEM images of the separated ND-Ox in typical fractions (scale bar: 50 nm). D) UV-Vis absorption spectra of the four fractions.